Ultrasound Piezo-Disk Transducer Model for Material Parameter Optimization

Lorenzo Spicci and Marco Cati
Research and Development Department, Esaote S.p.A., Via di Caciolle 15, 50127, Florence, Italy.
lorenzo.spicci@esaote.com, marco.cati@esaote.com

Abstract: The technology involved in high performance ultrasound imaging probes needs a reliable model to help in new projects development and performance simulations.

To achieve a useful model, it is necessary to use correct values for all material parameters involved in the electro-acoustical performances of the piezoelectric material, but unfortunately some of these parameters are known only with high uncertainty and others are not always present in the manufacturer specifications.

The present work consists in the development of a simple Finite Elements Model (FEM) for a piezoelectric disk transducer, along with a reliable optimization procedure to determine all parameters for the materials involved in the transducer functioning.

The results presented here show that the optimized model can be used to predict measurements results in term of electrical impedance magnitude, frequency response and directivity of emission of the transducer with a high accuracy. Some other intermediate results are briefly discussed like radial resonance modes.

Keywords: ultrasound, piezoelectricity, FEM model, optimization procedures, COMSOL.

1. Introduction

Ultrasound imaging transducers are devices that generate a pressure field into the human body, according to an electrical signal [1]. The differences in acoustic properties of different types of tissue allow the scanner to generate an image of a part of the body, based on the echo signals. The quality of the resulting image is strictly related to the technology level of the materials involved in the transducer manufacturing and the understanding of their interactions. This is why a complete Finite Elements Model (FEM) for such a device can greatly help in the study and optimization of its electro-acoustical performances [2].

In the present work, a 12 mm diameter, 0.5 mm thick, PZT CTS 3203HD piezoelectric ceramic [3] disk has been used to manufacture a cylindrical disk transducer, with hard rubber backing substrate and one high density front matching layer. The cylindrical transducer has been used to compare all measured electro-acoustical parameters (i.e. electrical impedance, pressure field level, directivity) with those obtained by the axial-symmetric FEM simulation, which was developed in COMSOL Multiphysics® environment.

Our work was focused on an optimization procedure needed to determine all parameters involved in the transducer performances. This was achieved by a "*step approach*", consisting in the study, FEM simulation and optimization of the transducer, following its manufacturing stages.

The optimization procedure is based on the minimization of the root mean square deviation (RMS) of a specific objective function between measured and simulated physical quantities.

2. Governing Equation

2.1. Piezoelectricity equations in COMSOL

The constitutive equations for a piezoelectric material are [2], in *stress-charge* form :

$$\begin{cases} \mathbf{T} = \left[\mathbf{c}^{E}\right] \mathbf{S} - \left[\mathbf{e}^{t}\right] \mathbf{E} \\ \mathbf{D} = \left[\mathbf{e}\right] \mathbf{S} + \left[\boldsymbol{\varepsilon}^{S}\right] \mathbf{E} \end{cases} \quad (1)$$

where $\mathbf{T}$ is the stress vector, $\mathbf{c}$ is the elasticity matrix, $\mathbf{S}$ is the strain vector, $\mathbf{e}$ is the piezoelectric matrix, $\mathbf{E}$ is the electric field vector, $\mathbf{D}$ is the electric displacement vector, $\boldsymbol{\varepsilon}$ is the dielectric permittivity matrix. The superscripts indicates a zero or constant corresponding field. Equations (1) takes into account both piezoelectricity, both mechanical and electrical anisotropy of the material.

Once these matrices have been specified, COMSOL recognizes which equations and in which domain are to be used inside the FEM elements.

2.2. Acoustics equations in COMSOL

Pressure waves emitted from the piezoelectric transducer in a biological medium are solution to the wave equation (time domain):

$$\nabla^2 p(r,t) - \frac{1}{c^2}\frac{\partial^2 p(r,t)}{\partial t^2} = 0 \qquad (2)$$

where $p(r,t)$ is the pressure and c is the speed of sound in the medium.

It is possible to identify two significant regions where wave propagation characteristics are very different: near field and far field region [1]. As regard our study, the region of interest is the far field, where waves are locally planar, velocity and pressure are in phase and the pressure amplitude drops at a rate inversely proportional to the distance from the source.

For homogeneous media, the solution of (2) can be written as a boundary integral (*Helmholtz-Kirchhoff*) anywhere outside a closed surface S containing all sources, in terms of quantities evaluated on the surface [4] (frequency domain):

$$p(\mathbf{R}) = \frac{1}{4\pi}\int_S \frac{e^{-jk|\mathbf{r}-\mathbf{R}|}}{|\mathbf{r}-\mathbf{R}|}\left(\nabla p(\mathbf{r}) + p(\mathbf{r})\frac{1+jk|\mathbf{r}-\mathbf{R}|}{|\mathbf{r}-\mathbf{R}|^2}(\mathbf{r}-\mathbf{R})\right)\cdot \mathbf{n}\, dS \quad (3)$$

where k is the wave number, $\mathbf{R}$ is the vector distance between observation point and reference system origin, $\mathbf{r}$ is the vector distance between observation point and source, $\mathbf{n}$ is the normal vector pointing into the domain that S encloses.

Starting from (3), if the surface S has an axially symmetric geometry, the pressure field level in the far field region $(|\mathbf{r}| \to \infty)$ can be approximated by [4] (neglecting the oscillating phase factor) :

$$p_{far}(\mathbf{R}) \approx -\frac{1}{2}\int_S r e^{jk\frac{zZ}{|\mathbf{R}|}}\left[\begin{array}{l} J_0\left(\frac{krR}{|\mathbf{R}|}\right)\nabla p(\mathbf{r})\cdot\mathbf{n} - \\ \frac{jkp(\mathbf{r})}{|\mathbf{R}|}\left(j\mathbf{n}_r R J_1\left(\frac{krR}{|\mathbf{R}|}\right) + \mathbf{n}_z Z J_0\left(\frac{krR}{|\mathbf{R}|}\right)\right)\end{array}\right] dS \quad (4)$$

where J_0, J_1 are Bessel functions of order 0 and 1 respectively, r and z are the radial and axial components of $\mathbf{r}$, R and Z are the radial and axial components of $\mathbf{R}$, $\mathbf{n}_r$ is the normalized vector in r direction, $\mathbf{n}_z$ is the normalized vector in z direction.

If the piezodisk is placed in $z = 0$ and the integration surface S is taken in the same plane, most of the terms in (4) cancel out and we can express the pressure p only in term of the angular coordinate ϑ [5]:

$$p(\vartheta) = \int_S r J_0\left(kr\sin(\vartheta)\right)\frac{\partial p}{\partial z}dr \qquad (5)$$

This integral has been used in COMSOL as integration variable, in order to use the optimization module with objective function given by the difference of measured and simulated on-axis pressure level.

The (Sound) pressure level is defined by:

$$L_p = 10\log_{10}\left(\frac{1}{2}\frac{p\cdot p^*}{p_{ref}^2}\right) \qquad (6)$$

Where p_{ref} is the "zero" reference sound pressure in air, with a value of 20μPa RMS, which is considered the threshold of human hearing (at 1 kHz) and p^* is the complex conjugate of pressure p.

2.3. Electric equations in COMSOL

The electrical impedance Z of a piezoelectric disk can be expressed by the general ohm law:

$$Z = \frac{V}{I} \qquad (7)$$

where V is the potential difference voltage across the two disk faces and I is the current flowing inside.

As regard the electric current flowing in the disk, the following integral holds (axial symmetry):

$$I = \int_0^r j_z(r)\, 2\pi r dr \qquad (8)$$

where $j_z(r)$ is the current density component along z axis.

This integral has been used in COMSOL as integration variable, in order to use the optimization module with objective function given by the difference of measured and simulated electrical impedance.

3. Piezoelectric Disk Transducer

3.1. Transducer assembly

The piezoelectric disk transducer was built with top quality manufacturing procedures, in order to have the best comparison with model simulation.

In order to work as an imaging transducer, the piezoelectric material needs to be bond on a backing substrate material which acts not only as a support, but also as an efficient damper for the back-traveling pressure wave: an high density ($3700 g/cm^3$) rubber was chosen.

On the other hand, a tungsten-powder-loaded epoxy was bond in front of the ceramic, acting as acoustic impedance matching layer, between high impedance ceramic (30-35 MRayls) and low impedance acoustic medium (i.e. human tissue, ~1.5 MRayls). These two materials are modeled in COMSOL by entering the Young modulus, Poisson ratio and density respective values.

Figure 1 is a picture of the transducer.

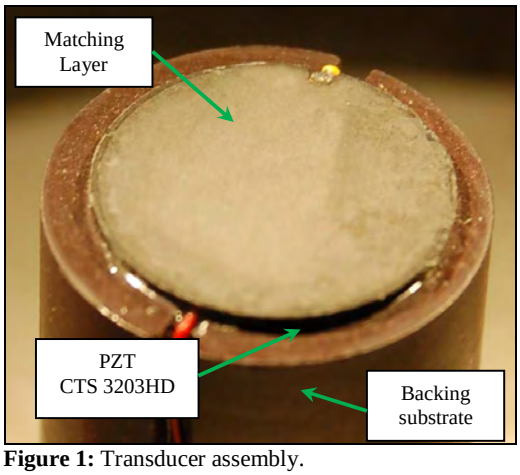

Figure 1: Transducer assembly.

3.2. Transducer characterization through measurements

The transducer's fundamental performances can be evaluated by measurement of electrical impedance and far field pressure level; whose quality and reliability play an important role in the comparison with simulation results. For this purpose it is very important to minimize all the parasitic effects which could result in a misleading measurement.

In the case of electrical impedance measurement, a minimum length twisted connection wires as been used, to avoid resonance frequency shift due to parasitic inductance effects.

Moreover, in the case of pressure field measurements it is important to measure also the effective driving voltage on the transducer terminal since the high capacitance transducer loads the waveform generator output in a way that the generator voltage is reduced. This data must be used in the FEM (see following).

As regard other measurement details, we have used general purpose instrumentations (Hewlett Packard 4195A Network Analyzer, Agilent 33250A waveform generator, LeCroy LT342 oscilloscope) and an high bandwidth membrane hydrophone placed in a thermostated, demineralized water tank (Figure 2).

Finally, great care must be used to place the hydrophone in the far field region and aligning it perpendicular to the transducer axis until the signal is maximized.

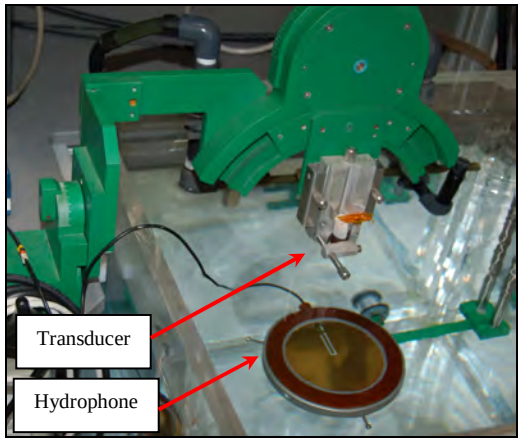

Figure 2: Measurement setup.

4. Use of COMSOL Multiphysics

4.1. Building the model

The transducer's model was built using the COMSOL Acoustics module, coupling the Piezo Axial Symmetry and Pressure Acoustics applications. Then, the Optimization module was

used to fit the model simulation to the measurement results.

The transducer was built with 2D axial symmetry and mesh on all domains was choosen as free tetrahedral. In order to consider a quasi-static approximation for each elementary triangular element, the segment length should be shorter than approximately $\lambda/5$[1]. This permits a good compromise between computational time and accuracy results.

In order to reduce the complete FEM node number, the acoustic domain (i.e. water) was reduced to a small region surrounded by Perfectly Matched Layer (PML), which simulate the zero reflection condition. Then far field pressure was calculated, as previously discussed. Figure 3 shows the implemented FEM.

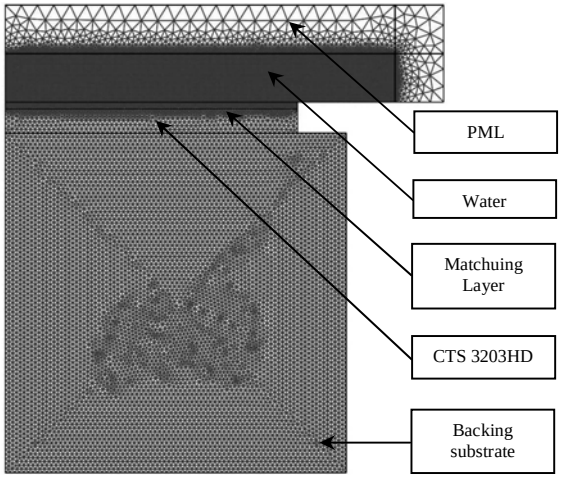

Figure 3: COMSOL FEM.

4.2. Optimization *step approach*

Due to the large number of parameters to be determined, we decided to follow a *step approach* procedure, summarized in the following:

1) Simulation and measurements for the piezoceramic disk alone.
2) Simulation and measurements for the piezoceramic disk bonded on backing substrate.
3) Simulation and measurements for the complete transducer: piezoceramic disk, backing substrate and front matching layer.

For each of the step above, the optimization is based on RMS minimization for the objective function given by the difference between measured and simulated electrical impedance, as reported in §2.3.

5. Results

We present here the results obtained for the electrical impedance and pressure field level, after the optimization procedure was performed.

5.1. Piezoelectric disk alone

A frequency response analysis was performed, between 1 MHz and 7 MHz. The optimization procedure for the electrical impedance was performed as described in the previous paragraphs. The measured (solid line) and simulated (dotted line) results are reported in Figure 4.

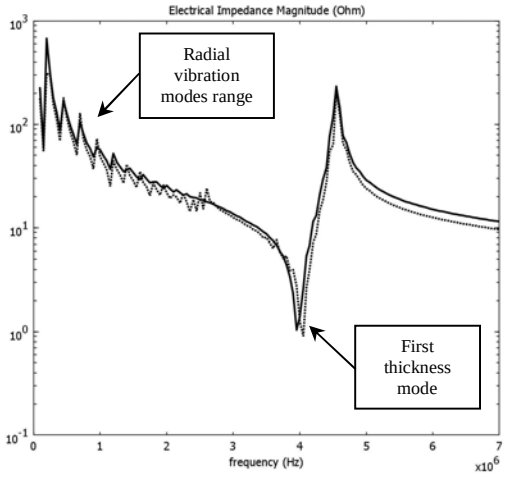

Figure 4: Piezoceramic electrical impedance magnitude (log scale): measured (solid) and simulated (dotted).

The agreement between measurements and simulation results is good over the whole frequency range. In particular, resonance and antiresonance frequency fit error is about 3%.

Both first thickness vibration mode (4 MHz) and radial vibration modes (from 150 kHz up to 2.5 MHz) can be clearly recognized. Note that the radial mode frequency sequence satisfies the zeros and poles sequence of the equivalent transmission line, which has a length proportional to the disk radius.

[1] If the hardware constraints (memory, CPU speed) allow it, an element size of $\lambda/10$ is preferred.

Going back to the optimization procedure, in COMSOL environment it is possible to verify that some material parameters are more critical than other in the optimization process. In Table 1 we report the list of tested parameters, along with the effect of each one on the electrical impedance response. The third column contains the range of frequencies where maximum sensitivity to the listed parameter variations was observed. Note that it is important to perform an individual optimization procedure for each parameter, focusing only within this range, in order to get solution convergence and sensible results.

Table 1: critical parameter and specific region of influence on the electrical impedance response.

Parameter	**Relevant changes on electrical impedance magnitude**	**Optimization frequency range**
c_{33} (Elasticity matrix)	Resonance and antiresonance freq. and amplitude of first thickness vibration mode	Neighborhood of first thickness mode resonance
e_{33} (Piezoelectric matrix)	Antiresonance freq. and amplitude of first thickness vibration mode	Neighborhood of first thickness mode antiresonance
ε_{33} (Dielectric matrix)	Antiresonance freq. and amplitude of first thickness vibration mode	Neighborhood of first thickness mode antiresonance
$c_{11}, c_{22}, c_{13}, c_{23}$ (Elasticity matrix)	Resonance and antiresonance freq. and amplitude of radial vibration modes	Neighborhood of first radial mode resonance
e_{15} (Piezoelectric matrix)	Antiresonance freq. and amplitude of radial vibration modes	Neighborhood of first radial mode resonance
α_{Piezo} (Rayleigh damping coeff.)	Radial vibration mode amplitude (lower freq.)	Neighborhood of first radial mode resonance
β_{Piezo} (Rayleigh damping coeff.)	Thickness vibration mode amplitude (higher freq.)	Neighborhood of first thickness mode antiresonance

In order to confirm the vibration mode characteristics, it's possible to check the deformed shape animation for a fixed frequency. This was done for the first thickness vibration mode (4 MHz, Figure 5) and for the first radial vibration mode (150 kHz, Figure 6).

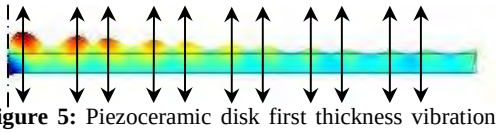

Figure 5: Piezoceramic disk first thickness vibration mode (4.0 MHz), *z-r* plane view.

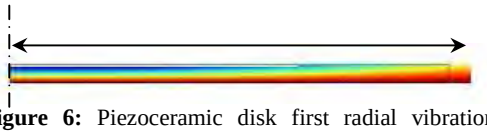

Figure 6: Piezoceramic disk first radial vibration mode (150 kHz), *z-r* plane view.

5.2. Piezoelectric disk with backing substrate

After the piezoceramic was studied, the backing substrate was added and another optimization procedure performed. The final result for the electrical impedance is shown in Figure 7 (solid line: measured, dotted line: simulated).

Again, fit to measurements is good, with resonance (~3.8 MHz) and antiresonance frequency (~4.7 MHz) error below 3%. Moreover, as expected, the quality factor at the resonance frequency is reduced and radial modes are almost cancelled by bonding on backing substrate material.

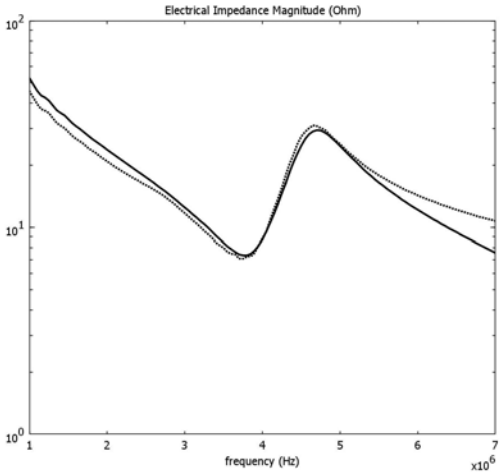

Figure 7: Piezoceramic disk with backing substrate electrical impedance magnitude: measured (solid) and simulated (dotted).

As in the previous case, the backing substrate parameters influence the electric impedance response. Table 2 is organized in the same way of Table 1 (§5.1).

Table 2: Backing substrate parameters optimization.

Parameter	Relevant changes on electrical impedance magnitude	Optimization frequency range
$E_{Backing}$ (Backing substrate Young Module)	Thickness vibration mode amplitude	Neighborhood of first thickness mode antiresonance
$\nu_{Backing}$ (Backing substrate Poisson coeff.)	Thickness vibration mode amplitude	Neighborhood of first thickness mode antiresonance
$\beta_{Backing}$ (Backing substrate Rayleigh damping coeff.)	Smoothen all trace	Neighborhood of first thickness mode antiresonance
ε_{33} (Dielectric matrix)	Bonding to backing lower piezoceramic capacitance	Neighborhood of first thickness mode antiresonance

5.3. Complete transducer (Piezoelectric disk with backing substrate and front matching layer)

Finally the front matching layer was added and the optimization procedure performed again. The final result in term of electrical impedance is shown in Figure 8 (solid line: measured, dotted line: simulated).

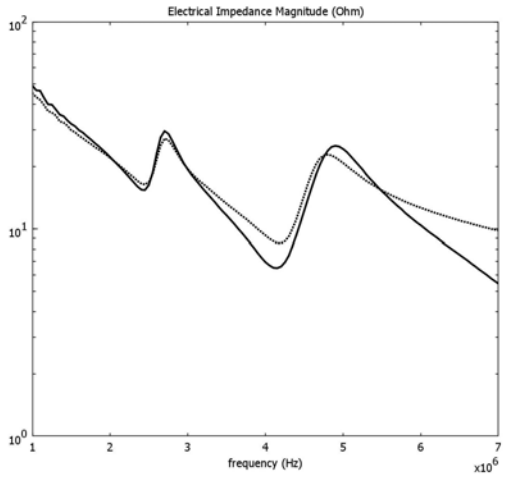

Figure 8: Complete transducer electrical impedance magnitude: measured (solid) and simulated (dotted).

Again, fit to measurements is quite good, with resonance and antiresonance frequency error below 5%. Moreover, both resonance due to piezoceramic (~4.1 MHz) and resonance due to matching layer (~2.4 MHz) are clearly visible.

As in the previous case, the matching layer parameters influence the system response. These are reported in Table 3, which is organized in the same way of Table 1 (§5.1).

Table 3: Matching layer parameters optimization.

Parameter	Relevant changes on electrical impedance magnitude	Optimization frequency range
$E_{Matching\ Layer}$ (Matching Layer Young Module)	Resonance freq. and amplitude due to the matching layer	Neighborhood of matching layer resonance (2.5MHz)
$\nu_{Matching\ Layer}$ (Matching Layer Poisson coeff.)	Resonance freq. due to the matching layer	Neighborhood of matching layer resonance (2.5MHz)
$\beta_{Matching\ Layer}$ (Matching Layer Rayleigh damping coeff.)	Resonance amplitude due to the matching layer	Neighborhood of matching layer resonance (2.5MHz)

With the complete FEM (§4.1), the pressure field generated by the transducer was studied.

The frequency response analysis was run using the measured driving voltage as electrical boundary condition for the disk. The far field pressure level was calculated as explained in §2.2. In this last step the optimization process was based on the RMS difference between measured and simulated far field pressure level, calculated as in (5). No improvement with respect to the results obtained with electrical impedance optimization was observed.

Figure 9 shows the comparison in terms of far field pressure level between measured results (solid line) and simulated results (dotted line). In this case we obtain a discrepancy of less than 5% error in maximum amplitude frequencies and less than 1dB in corresponding amplitude values, with respect to measurements.

As a final check of the model efficiency, the directivity performance of the transducer was both measured and simulated, at 3 MHz operating frequency. This frequency corresponds to the first maximum of the emitted pressure field level (see Figure 9).

Figure 10 shows the comparison in terms of far field directivity between measured result (solid line) and simulated result (dotted line). Also in this case the agreement between measurement and simulation is good, with less than 5% amplitude error at -6dB from maximum.

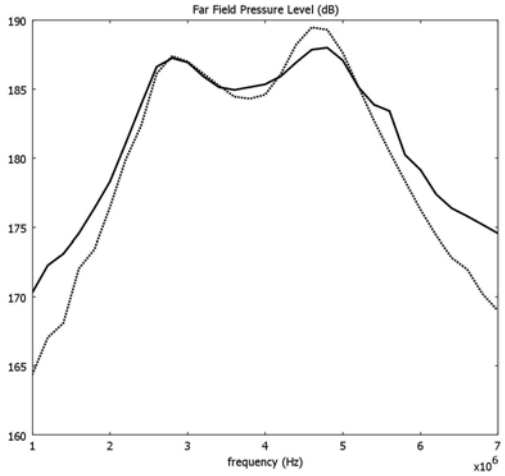

Figure 9: Far field pressure level (dB): measured (solid) and simulated (dotted).

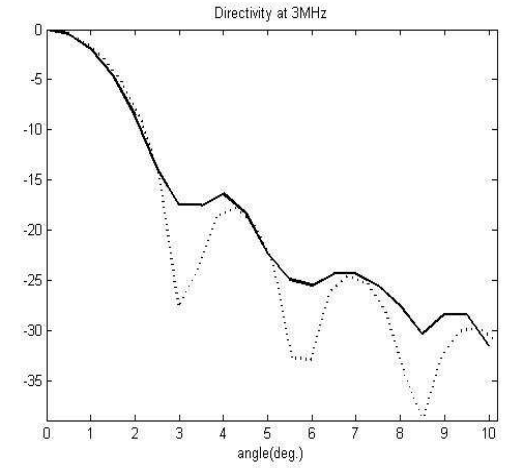

Figure 10: Far field directivity (dB): measured (solid) and simulated (dotted).

6. Conclusions and future work

A Finite Element Model (FEM) for an ultrasound piezoelectric transducer has been developed. The FEM design follows a "*step approach"* which consists in the development of the model along with the transducer manufacturing stages, starting from the choice of ceramic piezoelectric material, up to the complete transducer assembly (piezoceramic, backing substrate and front matching layers).

Final results for the far field pressure level show a good agreement between measured and simulated transducer performances, corresponding to 5% error in maximum amplitude frequencies and less than 1dB in the amplitude values. Better results are obtained in terms of electric impedance where an error within 3% in resonant frequencies and amplitudes are achieved.

Moreover, taking advantage of the simplicity of the problem under study, it was quite easy to establish an optimization procedure that could be followed for future works. These will be the development of models for imaging probe arrays, with much more complicated geometries and operating conditions.

7. References

[1] Peter Fish, "*Physics and Instrumentation of Diagnostic Medical Ultrasound*", Wiley, June 1990

[2] N. N. Abboud, *et alii*, "*Finite Element Modeling for Ultrasonic Transducers*", SPIE Int. Symp. Medical Imaging 1998

[3] S. Sherrit, *et alii*, "*A complete characterization of the piezoelectric, dielectric, and elastic properties of Motorola PZT 3203 HD including losses and dispersion*", SPIE, Vol. 3037, Feb 1997

[4] COMSOL Multiphisics Acoustic Module User Guide, ver.3.5a, pages 32-33

[5] COMSOL Multiphisics Model Documentation, "*Optimizing the Shape of a Horn*", Model ID 4353.